



Published in final edited form as:

Stem Cells. 2006 November ; 24(11): 2504–2513. doi:10.1634/stemcells.2006-0119.

Axonal Growth Regulation of Fetal and Embryonic Stem Cell-Derived Dopaminergic Neurons by Netrin-1 and Slits

Ling Lin and Ole Isacson

Udall Parkinson's Disease Research Center of Excellence and Neuroregeneration Laboratories, McLean Hospital/Harvard Medical School, Belmont, Massachusetts, USA

Abstract

The physical restoration of dopamine circuits damaged or lost in Parkinson disease by implanting embryonic stem (ES)-derived cells may become a treatment. It is critical to understand responses of ES-derived dopamine (DA) neurons to guidance signals that determine axonal path and targeting. Using a collagen gel culture system, we examined effects of secreted molecules Netrin-1 and Slits on neurite outgrowth of fetal DA neurons and murine ES-differentiated DA neurons. We have previously shown that fetal DA neurons express DCC and Robo1/2 receptors and that Netrin-1 and Slit2 function as an attractant and a repellent for DA neurite outgrowth. In the present study, we observe that both Slit1 and Slit3 repel and inhibit neurite growth of fetal DA neurons. Here, we also demonstrate that ES-differentiated neurons including DA neurons express the Netrin receptor DCC and Slit receptor Robo proteins. In the gel culture system of ES cells, Netrin-1 promoted neurite outgrowth mediated by DCC receptor, and Slit1 and Slit3 were inhibitory for neurite outgrowth through Robo receptors. Slit2 appeared to exert inhibitory as well as repulsive effects in the coculture assay. However, unlike fetal DA neurites, no directed neurite outgrowth was observed in the cocultures of ES-derived DA neurons with Netrin-1-, Slit1-, and Slit3-producing cells. The findings suggest that ES-derived DA neurons generated by current protocols can respond to guidance cues in vitro in a similar manner to fetal cells but also exhibit distinct responses. This may result from developmental differences generated by present in vitro methods of cell patterning or conditioning during ES cell differentiation.

Keywords

Embryonic stem cell; Axon guidance; Dopaminergic neuron; Netrin-1; Slit

Introduction

The use of embryonic stem (ES) cells may provide a method to replace lost neurons in neurodegenerative disorders and to rebuild neuronal connectivity to restore brain function; for example in Parkinson disease (PD). PD signs are caused by loss of the dopamine (DA) neurons in the ventral midbrain (VM). VM consists of substantia nigra (SN) (area A9) and ventral tegmental area (VTA) (area A10) that project to dorso-lateral (caudate putamen) and ventral striatum (nucleus accumbens), forming the nigrostriatal and mesolimbic pathway, respectively [1,2]. It is known that axonal growth and targeting are determined by a group of extracellular guidance molecules during central nervous system (CNS) development [3-6]. Success of the

Correspondence: Ling Lin, M.D., Ph.D., Neuroregeneration Laboratories, Mailman Research Center, 115 Mill Street, Harvard Medical School/McLean Hospital, Belmont, Massachusetts 02478, USA. Telephone: 617-855-2075; Fax: 617-855-2838; e-mail: llin@mclean.harvard.edu; or Ole Isacson, M.D. (Dr. Med. Sci), e-mail: isacson@hms.harvard.edu.

Disclosures The authors indicate no potential conflicts of interest.

cell therapy largely depends on whether the new cells are able to make connections with host cells precisely. We have previously demonstrated that *in vivo* guidance mechanisms instructing growth and targeting of the engrafted fetal cells are well preserved in the adult host brain [7-9]. However, molecular and cellular mechanisms by which the dopamine neurons find their paths and synaptic partners remain largely unknown. Nevertheless, we do know that the guidance families are expressed in the DA pathway, such as Netrin/DCC, Slit/Robo, Ephrin/Eph, and Semaphorin/Neuropilin [10-13]. In particular, expressions of *Netrin-1* and *DCC* genes are observed in embryonic as well as adult nigrostriatal pathway [10]. Both *Robo1* and *Robo2* genes are found in the developing VTA and SN areas [12]. *Slit1* is highly expressed in the embryonic striatum, and the expression is much decreased in the adult striatum [12]. *Slit3* expression appears in the striatum at postnatal day 5 and increases in the adult striatum, and *Slit2* is expressed in the areas adjacent to striatum, such as cerebral cortex and septum [12]. Their roles in the establishment of the DA circuits have only recently been evaluated [11,14]. Studies from our group and others further demonstrated that fetal DA neurons of A9 and A10 preferentially innervate their normal territories when grafted in a PD patient and in a PD animal model [15,16], indicating that the fetal DA cells may use the same guiding molecules that determine the selective termination zones by A9 and A10 cells during development. However, transplants of ES cells into a PD animal model have produced distinct outcomes regarding DA neuron survival, axonal outgrowth, innervation, and functional recovery. Fetal tissue contains certain ratio of glial cells that are normally generated along with neurons. It is not known whether *in vitro* generated ES-derived neuronal mixtures have normal access to glial conditions necessary for differentiation and synaptic formation [17,18]. This may account for some differences in outcomes between fetal and ES-induced neurons both *in vitro* and *in vivo*. Striatal implantation of undifferentiated D3 ES cells leads to behavioral restoration of DA-mediated motor asymmetry accompanied by fully developed DA neurons that integrated well with the host [19]. However, transplantation of differentiated murine ES cells can result in some behavioral recovery even with limited axonal outgrowth and integration [20]. Grafting of a primate ES cell line also shows a long-term survival of DA neurons with limited axonal outgrowth [21]. A lack or minimal survival of grafted DA neurons differentiated from human ES cells has been reported in a rodent PD model [22,23]. There are differences between cell composition of fetal and ES-derived DA-enriched grafts; although the ES-differentiated DA neurons appear to possess nearly all the essential genetic and molecular properties *in vitro*. Fetal transplants contain normally developed DA cells and surrounding cells that are isochronically generated, whereas *in vitro* ES-derived neurons are artificially induced and grow with developmental atypical cell types, multiple cell types, some of which are non-neural and some of which are immature [21]. This could result in differences between fetal and ES-derived transplants in cell survival, axonal growth and integration. A study using fetal VM cells and ES-differentiated neurons has provided morphological and functional comparison of these two types of neural grafts [24]. This study shows survival of comparable numbers of DA neurons, but only fetal DA neurons grow abundant neurites that improve motor dysfunction [24], indicating that in this case, distinct interactions of the cells with the host may account for the outcomes. For reestablishing DA circuits, the basic question to ask is whether ES-derived neurons are capable of interacting with the guidance cues located in the adult targets.

The present *in vitro* study examined whether ES-differentiated DA neurons express guidance molecule receptors present in the fetal DA cells and determined responses of ES-derived DA neurons to secreted guidance factors Netrin-1 and Slits, which are expressed by striatal cells using a collagen gel culture system. These experiments provide basic information about similarities and differences between fetal and ES-derived DA neurons in response to guidance factors.

Materials and Methods

Animals

All animal studies were carried out following National Institutes of Health guidelines and were approved by the Institutional Animal Care and Use Committee at McLean Hospital, Massachusetts General Hospital, and Harvard Medical School. Time-pregnant Sprague-Dawley rats at embryonic day 14 (E14) were obtained from Charles River Breeding Laboratories (Wilmington, MA, <http://www.criver.com>). The day on which a vaginal plug was found was considered E0.

Embryonic Stem Cell Culture

All culture media were purchased from Invitrogen (Grand Island, NY, <http://www.invitrogen.com>), and all other products were obtained from Sigma-Aldrich (St. Louis, <http://www.sigmaaldrich.com>) unless otherwise specified. We used D3 mouse embryonic stem cell (American Type Culture Collection, Manassas, VA, <http://www.atcc.org>) and PA6 stromal cell (Riken, Tsukuba, Japan, <http://www.riken.go.jp>) as feeder and followed the culture procedure developed by Kawasaki et al. [25]. We have previously demonstrated that using this method, D3 ES cell-differentiated dopamine neurons (approximately 30% of total neurons) display a mesencephalic phenotype, including gene expressions of dopamine transporter, aromatic L-amino acid decarboxylase, Ptx3, and aldehyde dehydrogenase [26]. PA6 cells were grown on coverslips precoated with 1% gelatin in 24-well plate filled with Dulbecco's modified Eagle's medium (DMEM) supplemented with 10% FBS and antibiotics. Single D3 cells were seeded on confluent PA6 monolayer at a density of 1.5×10^3 cells per coverslip and were grown with a differentiation medium containing 10% knockout serum replacement, 2 mM glutamine, 1 mM pyruvate, 0.1 mM nonessential amino acids and 0.1 mM 2-mercaptoethanol (2-ME) in Glasgow minimum essential medium (G-MEM) for 8 days. Then the growing medium was changed to G-MEM supplemented with N2, 1 mM pyruvate, 2 mM glutamine, 0.1 mM nonessential amino acids, and 0.1 mM 2-ME, and the culture was continued for 4 days.

Preparation of Cell Aggregates Expressing Netrin-1 and Slit1–3

Aggregates were generated as described previously [14]. Briefly, 293-Epstein-Barr virus nuclear antigen (EBNA) cells stably secreting recombinant chicken Netrin-1 protein (kindly provided by Dr. Marc Tessier-Lavigne, University of California, Stanford, CA) were cultured in DMEM containing 10% fetal bovine serum, 2 mM glutamine, 200 μ g/ml Hygromycin B (Boehringer Mannheim, Mannheim, Germany, <http://www.boehringer.com>), 250 μ g/ml Geneticin (Gibco-BRL, Gaithersburg, MD, <http://www.gibcobl.com>) and antibiotics. The 293-EBNA cell line transfected with control vector plasmid was used as control. For the Slit2 study, a stable 293-human embryonic kidney (HEK) cell line that secretes human Slit2 protein or control cells transfected with vector plasmid was cultured in DMEM containing 10% fetal bovine serum and antibiotics as described previously [14,27]. Cells secreting Slit1 and Slit3 molecule were generated by transfecting 293T cells with Slit1 and Slit3 plasmids (generous gifts from Dr. Yi Rao, Washington University, St. Louis) using Lipofectamine 2000 gene transfer method following the manufacturer's instructions. Transfection efficiency was monitored by transfection with green fluorescent protein plasmid and Western blots (data not shown). The cells were cultured with the growth media for 2 days and then harvested, centrifuged, and resuspended in 100 μ l of medium containing 0.5 million cells. Cell aggregates were prepared by hanging drop methods [14]. Expression of Slit2 in the 293-HEK cell line has been previously demonstrated by Western blots [28,29]. Netrin-1 expression in the 293-EBNA-transfected cells has been previously shown [30].

Explant Culture Preparation

Explant culture of the ventral midbrain was prepared from E14 rat embryos. The ventral midbrain was dissected out and cut into small squares in cold DMEM/Ham's F-12 medium. For ES cell explant culture, D3 colonies were dissected out at day 12 in vitro (Fig. 1). VM squares and ES colonies were transferred into 35- × 10-mm culture dishes. Collagen solution was prepared by mixing rat-tail collagen type 1 (BD Biosciences, Bedford, MA, <http://www.bdbiosciences.com>) with minimal essential medium. Collagen solution was pipetted onto the bottom of the dishes and allowed to gel, followed by adding a growth medium of DMEM/Ham's F-12 medium supplemented with 10% fetal bovine serum and antibiotics. To determine the effects of Netrin-1 on ES-derived axonal growth, a recombinant Netrin-1 (R&D Systems Inc., Minneapolis, <http://www.rndsystems.com>) was applied to the medium at 100–400 ng/ml. The concentration of netrin-1 chosen was based on a previous study showing that netrin-1 between 100 and 400 ng/ml promoted axonal growth [31]. To determine whether netrin-1 promoting activity for tyrosine hydroxylase (TH) neurite outgrowth required DCC receptor, a blocking antibody against DCC (clone AF5; Oncogene, San Diego, <http://www.oncogene.com>) was added to cultures at 10 μg/ml [14,32-34]. Species-matched immunoglobulin was used as control. When preparing the coculture of VM and ES explants with cell aggregates, cell aggregates were positioned 50–200 μm apart. For function-blocking experiments of Slit family, conditioned medium collected from confluent cultures of the 293-HEK cells expressing extracellular domain of Robo (RoboN) was added into culture medium at dilutions of 1:5 in the VM cocultures with Slit1 and Slit3 cells. This concentration was shown to reverse the inhibitory activity of Slit2 in our previous study [14]. RoboN carries hemagglutinin molecule and can bind to Slit molecules but is not able to stimulate the signaling pathway [28]. RoboN has been used as a competitive blocker for Slit-induced activities [27, 35]. For cocultures of ES cells with Slit2, RoboN was added to culture at dilutions of 1:3, 1:1, and 1:0. Cultures were placed in a humidified incubator at 37°C with 5% CO₂ for 1.5 days and were then fixed with 4% paraformaldehyde in 0.1 M phosphate buffer (pH 7.4) for 30 minutes at room temperature.

Immunofluorescence

Routine immunohistochemistry was performed in ES and explant cultures [14]. In brief, coverslips and explants were pretreated with 10% normal donkey serum (Jackson Laboratory, Bar Harbor, ME, <http://www.jax.org>) and 0.1% Triton X-100 in 0.1 M phosphate-buffered saline for 1 hour at room temperature, followed by incubation with primary antibodies at 4°C overnight and then with appropriate secondary antibodies conjugated with distinct fluorescence at room temperature for 1 hour. Antibodies against DCC (1:50; BD Pharmingen, San Diego, <http://www.bdbiosciences.com/pharmingen>), β III tubulin (Tuj1) (1: 2,000; Covance, Princeton, NJ, <http://www.covance.com>), TH (1:300; Pel-Freez, Rogers, AK, <http://www.pel-freez.com>) were used. Antibodies against Robo1 and Robo2 (1:50; Santa Cruz Biotechnology Inc., Santa Cruz, CA, <http://www.scbt.com>) used in the study have been shown to be specific [14,36]. Secondary antibodies conjugated with Alexa 488 and 568 (1:500; Molecular Probes Inc., Eugene, OR, <http://probes.invitrogen.com>) and Cy5 (1:100; ImmunoResearch Laboratories Co., West Grove, PA, <http://www.jacksonimmuno.com>) were used. Omission of primary antibodies or antibodies preincubated with excess antigens were served as control. Fluorescent signal was examined by a confocal imaging system (LSM510 META; Carl Zeiss, Thornwood, NY, <http://www.zeiss.com>).

Quantitative and Statistical Analyses

The area occupied by Tuj1-positive neurites in the ES explants was highlighted by a function of threshold and measured using MetaMorph software (Universal Imaging Corp., Downingtown, PA, <http://www.moleculardevices.com>). For ES explant cocultures,

MetaMorph was used to measure the area covered by Tuj1 neurites in proximal (P) or distal (D) aspect of the explants, and P/D ratio was therefore calculated in those experiments [14]. In the proximal explants of ES cocultures with Slit2 cells, neurites that stopped at one-third of the distance to the Slit2 aggregates were scored as “stop,” and neurites that turned away before reaching Slit2 aggregate area were considered “turn.” Those responding neurites were calculated as the percentage of total neurites in the proximal explants. For TH-positive neurites in the VM and ES cocultures, numbers of neurites and fascicles from proximal or distal aspect of the explants cultured with cell aggregates were counted at $\times 10$ using NeuroLucida (MicroBrightfield, Inc., Williston, VT, <http://www.microbrightfield.com>). TH neurite length in all cultures was measured using NeuroLucida. Statistical analyses were carried out using InStat software (GraphPad, Inc, San Diego, <http://www.graphpad.com>). $p < .05$ was considered significantly different.

Results

Expression of DCC and Robo1 and Robo2 Receptor Proteins in ES-Derived Neurons

We determined whether ES-differentiated neurons, and particularly dopaminergic neurons, expressed DCC and Robo1 and Robo2 proteins (receptors for ligand netrins and Slits, respectively). Immunohistochemistry showed that DCC receptor was expressed both in Tuj1-positive and TH-positive neurons (Fig. 1A–1D). We also observed that Robo1 and Robo2 receptors were expressed by both TH neurons and non-TH neurons (Fig. 2). This observation suggests that ES-differentiated neurons could interact with cognate guidance cues as grafted in the brain.

Effects of Netrin-1 on Neurite Outgrowth

In our previous study, we found that Netrin-1 protein promoted neurite outgrowth of the TH neurons derived from fetal mesencephalon [14]. Here, we tested whether ES-derived neurons could also respond to Netrin-1. Netrin-1 protein was added to the medium of explant culture at concentrations of 100 ($n = 21$), 200 ($n = 21$), 300 ($n = 24$), and 400 ($n = 34$) ng/ml. Explants cultured in the absence of Netrin-1 served as controls ($n = 39$). It appeared that explants in the presence of Netrin-1 at 300–400 ng/ml grew more neurites compared with other groups (Fig. 3A–3D). Because nearly all of the neurons express DCC receptor including TH neurons, we quantified the Tuj1 neurite outgrowth by measuring area occupied by Tuj1 neurites using MetaMorph software as described previously [14]. Statistical analysis revealed that the area covered by neurites in the explants incubated with Netrin-1 at concentrations of 300 and 400 ng/ml was greater than that in control explants (Fig. 3I, *, $p < .05$; **, $p < .001$; Kruskal-Wallis test). In addition, TH neurite length was measured using NeuroLucida. The explants incubated with Netrin-1 at 300 ng/ml ($n = 26$) displayed longer TH neurite growth than control explants ($n = 17$). To determine whether DCC was required for the axon growth-promoting activity of Netrin-1, a DCC-blocking antibody AF5 was applied (10 $\mu\text{g/ml}$) 30 minutes before addition of Netrin-1 (300 ng/ml) to the cultures ($n = 25$). This antibody has been shown to inhibit the DCC-mediated effects [32–34]. Addition of control IgG was served as control ($n = 25$). TH neurite length in explants incubated with Netrin-1 was significantly higher than that in the explants cultured without Netrin-1, with control IgG, and with AF5 and Netrin-1 (Fig. 3J, *, $p < .05$; Kruskal-Wallis test).

Guidance Roles of Netrin-1 in ES-Derived Neurons

To evaluate possible chemotropic effects of Netrin-1 on ES-derived neurons, a collagen gel culture system was set up for cocultures of ES colony with cell aggregate secreting guidance cues (Fig. 1). This set of new experiments is compared with Netrin-1 attracting TH neurites from E14 VM explants [14] to that of ES-derived neurons (Fig. 4A, 4B). Tuj1 neurites grew homogeneously in the explants cultured with control aggregates ($n = 18$; Fig. 4C). Tuj1 neurite

distribution in the explant cultured with Netrin-1 secreting cells ($n = 17$) showed no differences from control explants. Quantification of neurite distribution was carried out by measuring area covered by Tuj1 neurites in the P and D quadrants. P/D ratio was then calculated. No difference in P/D ratios was detected between two groups (Fig. 4I, $p > .05$; Mann-Whitney test). For ES-derived TH neurites (Fig. 4E, 4F), the number of TH neurites was counted in the proximal and distal explants, and P/D ratio was calculated. No significant difference in P/D ratio was observed between control explants ($n = 14$) and explants cultured with Netrin-1 cells ($n = 20$) (Fig. 4I, $p > .05$). We thought that a reason for this could be that Netrin-1 cells did not produce enough Netrin-1 proteins to navigate neurite outgrowth. We therefore decided to add exogenous Netrin-1 protein to the cocultures at concentrations of 100, 200, 300, and 400 ng/ml. However, no directed neurite growth was observed in any of these groups (Fig. 4G, 4H). Nonetheless, neurite outgrowth appeared to be enhanced by Netrin-1 addition, consistent with previous experiments.

Effects of Slit1 and Slit3 on Neurite Growth of Fetal and ES-Derived Neurons

In this study, we examined the effects of Slit1 and Slit3 on neurite outgrowth derived from E14 VM and ES using the coculture system. The majority of TH neurites in the fetal VM explants cultured with Slit1 cells ($n = 27$) was observed in the distal aspect of the explants, which was different from neurite distribution pattern seen in the control explants ($n = 34$) (Fig. 5A, 5B). We then added conditioned medium containing RoboN (an inhibitor for endogenous Robo receptors) at 1:5 to culture medium ($n = 17$) (Fig. 5C). The concentration used was based on our previous study [14]. TH neurite length and the number of TH neurites in the proximal and distal fetal VM explants were counted and measured (as described in Materials and Methods). TH neurite lengths in the explants cultured with Slit1 cells were shorter than those in the control explants (Fig. 5J, *, $p < .001$), and RoboN treatments neutralized Slit1 inhibitory activities (Fig. 5J, $p > .05$ compared with control; Kruskal-Wallis test). P/D ratio in the presence of Slit1 was lower than that in control explants and explants cultured with Slit1 cells and RoboN addition (Fig. 5K, *, $p < .001$, Kruskal-Wallis test). Similar results were observed in the cocultures of fetal VM with Slit3 cells (Fig. 5D–5F). TH neurite lengths in the explants cultured with Slit3 ($n = 30$) were significantly reduced compared with control explants ($n = 34$), and explants treated with RoboN at 1:5 ($n = 17$) (Fig. 5J, *, $p < .001$). The P/D ratio was significantly lower in the explants cultured with Slit3 cells compared with control explants (Fig. 5K, *, $p < .01$). Addition of RoboN reversed this asymmetric neurite distribution (Fig. 5K), proving that this effect was mediated by Robo receptors.

In the ES explants cultured with either control cells ($n = 27$) or Slit1-producing cells ($n = 30$) and Slit3-producing cells ($n = 27$) (Fig. 5G–5I), TH neurite lengths were reduced in explants cultured with Slit1 or Slit3 cells compared with length in the control explants (Fig. 5L, *, $p < .03$ for Slit1; *, $p < .002$ for Slit3; Mann-Whitney test). However, P/D ratios of the TH neurites did not differ between control explants and explants cultured with Slit1 or Slit3 cells (Fig. 5M, $p > .05$; Mann-Whitney test). In addition, Tuj1 neurites grew homogeneously but displayed short length in the explants incubated with Slit1 ($n = 33$) and Slit3 cells ($n = 29$) compared with control explants ($n = 33$) (Fig. 6A–6C). The areas covered by Tuj1 neurites were significantly reduced in the cocultures of ES with Slit1 or Slit3 cells compared with control cocultures (Fig. 6D, *, $p < .0001$; Mann-Whitney test). In contrast, P/D ratios were not statistically different between control explants and explants cultured with Slit1 or Slit3 cells (Fig. 6E, $p > .05$; Mann-Whitney test).

Effects of Slit2 on Neurite Growth of ES-Derived Neurons

It has been shown that Slit2 inhibits neurite outgrowth in the DA pathway [14]. Its effects on the neurite outgrowth of ES-derived neurons, including DA neurons, are unknown. We evaluated Slit2 functions in regulating Tuj1 and TH neurite outgrowth of ES-differentiated

neurons using the coculture system. In the explants cultured with control cells ($n = 12$), the neurite grew homogeneously (Fig. 7A). In contrast, the neurite distribution pattern appeared disrupted in explants cultured with Slit2 cells ($n = 12$) (Fig. 7B). Fewer neurites were seen in the explants grown next to Slit2 cells. RoboN was added to the cultures at dilution of 1:3, 1:1, and 1:0 ($n = 8, 10, \text{ and } 7$, respectively) (Fig. 7C, 7D). We then counted neurites that turned away from the Slit2 cell aggregates and stopped extending at the proximal part of the explants; these data are presented as percentage turn and stop of total neurites in the proximal explants to Slit2 cells (Fig. 7G). The ratio of turned and stopped neurites was greater in explants cultured with Slit2 cells compared with controls, and only RoboN at a dilution of 1:0 reversed such effects (*, $p < .01$, control vs. Slit2, RoboN 1:3, and 1:1; $p > .05$, control vs. RoboN 1:0; Kruskal-Wallis Test).

A number of TH neurites were observed in the explants cultured with control cells ($n = 9$; Fig. 7E), whereas explants cultured with Slit2 cells ($n = 12$) showed fewer TH neurites (Fig. 7F). Significant reduction of TH neurite outgrowth was observed in the explants cultured with Slit2 cells compared with control explants, and RoboN (1:0) treatment ($n = 10$) neutralized such inhibitory effects of Slit2 on TH neurites (Fig. 7H, *, $p < .05$, Slit2 vs. control or RoboN treatment; $p > .05$, control vs. RoboN 1:0; Kruskal-Wallis Test).

Discussion

We established a gel explant culture system that allowed us to examine the influence of guidance cues on axonal outgrowth of fetal midbrain DA neurons and ES-derived DA neurons. In fetal VM cocultures with Netrin-1 and Slit2 cell aggregates, we previously found that Netrin-1 attracts and Slit2 repels TH neurite outgrowth [14], and in the present study, we further observed that Slit1 and Slit3 were inhibitory and repulsive for the neurite growth of fetal midbrain DA neurons. We also observed that guidance receptors DCC and Robo1 and 2 proteins were expressed by ES-derived TH neurons and also non-TH neurons. Netrin-1 protein promoted neurite outgrowth including TH neurites, mediated by the DCC receptor. Slit1 and Slit3 inhibited overall neurite extension, and Slit2 appeared to repel and inhibit neurite outgrowth of ES-derived neurons. However, no directed TH and Tuj1 neurite outgrowth was seen in the cocultures of ES-derived neurons with Netrin-1 and Slit1 and Slit3 cells. These observations demonstrate that ES-differentiated DA neurons can respond to the typical guidance cues of in vivo developed fetal neurons but also exhibit significant differences in this culture system.

Netrin-1 Promotes Neurite Outgrowth of ES-Derived Neurons

The Netrin-1/DCC guidance pair elicits an axon outgrowth promoting activity and is required for development of many neural projections [37-40]. Our previous study showed that Netrin-1 via DCC receptor enhanced and attracted neurite outgrowth of the dopamine neurons derived from fetal ventral midbrain [14]. Persistent expression of Netrin-1/DCC is observed in adult SN and striatum, and grafted DA neurons derived from fetal grow specifically to the appropriate adjacent and distant target areas from ectopic and homotopic implantation sites [7-9]. Moreover, our group and others have demonstrated that engrafted fetal A9 and A10 cells differentially terminate axons into their normal territories [15,16]. These observations indicate that the guidance determinants are precisely preserved for new neurons to grow to their targets. Generally, guidance activities are spatiotemporally regulated events during CNS development, and expression of guidance cues disappears or is much reduced in the adult brain [10]. It is not known whether the new neurons can trigger or transiently stimulate expression of guidance molecules required for axon growth instruction. Nevertheless, Netrin-1 may play a part in regulation of DA axonal outgrowth and functions as a permissive cue for DA axons to find their target region in striatal grafts of fetal VM cells. Using our paradigm of ES explant cultures,

we found that Netrin-1 enhanced neurite outgrowth including DA neurite. However, we did not observe the expected guidance activity of Netrin-1 cells in this coculture system.

Effects of Slit1 and Slit3 on DA Neurite Outgrowth

Slit1 and Slit3 are members of the Slit family expressed by striatal cells in a developmentally regulated pattern [12]. Slit1 is highly expressed in the developing striatum and this expression is much reduced in the adult. In contrast, Slit3 expression emerges in striatum at postnatal day 5 and increases dramatically in the adult [12]. We have shown that Slit2 inhibits neurite extension and repels neurite outgrowth of fetal midbrain DA neurons [14]. In the present study, we found that both Slit1 and Slit3 were repulsive for fetal VM TH neurites and also functioned as inhibitors for DA neurite outgrowth observed in the coculture system. Using the current protocol and patterning for ES derivation of DA neurons, ES-differentiated DA neurons as well as non-DA neurons did not respond to the repulsive properties of Slit1 and Slit3 molecules, unlike fetal DA neurons. However, the neurite outgrowth of ES-derived DA neurons was indeed suppressed by Slit1 and Slit3 molecules, suggesting that Slit1 and Slit3 can also regulate ES-derived neuronal growth, and these inhibitory effects are important for axons to find appropriate termination zones.

Effects of Slit2 on Neurite Outgrowth of ES-Derived Neurons

In the coculture systems, neurite outgrowth from ES-derived neurons responded to Slit2 in two ways. First, neurites appeared to avoid Slit2 secreting cell aggregate causing asymmetric neurite distribution. Second, neurites facing Slit2 stalled in an area proximal to the explants. These results suggest that Slit2, unlike Slit1 and Slit3, exerted inhibitory as well as repulsive effects in this coculture assay. TH neurite outgrowth was also inhibited. These effects were mediated through Robo receptor because RoboN can neutralize such activities. Slit2 is a key chemorepellent for the developing axons and prevents commissural axons from recrossing the midline [41]. In addition, studies have shown that Slit2 are involved in axon pathfinding of forebrain and retinal ganglion neurons [42,43]. Slit2 can be proteolytically cleaved into 140-kDa N-terminal (Slit2-N) and 55–60-kDa C-terminal (Slit-C) fragments in vivo and in vitro, and only Slit2-N can stimulate axon branching of dorsal root ganglia, the nerve growth factor-responsive neurons but induces collapse of olfactory bulb axons [44,45]. These findings indicate that responses to Slit2 protein are fragment-specific and axon type-specific. However, it is still not clear what mechanisms cleave Slit protein and whether Slit-C has any biological role. Whether Slit1 and Slit3 can also be further cleaved remains to be determined.

In addition to Netrin/DCC and Slit/Robo guidance families, semaphorin/Neuropilin and Ephrin/Eph are expressed in the dopamine system [11], although their roles in guidance of DA neuronal growth have not been characterized. Growth factors, transcriptional regulators, morphogenes, and cell adhesive molecules can also be involved in distinct aspects of pathway specification and determination of axonal termination zones [46-48]. These factors may also have influences on axonal growth of fetal and ES-derived neurons in a cell-based therapy for PD and may contribute to normal axon pathfinding of ES-differentiated DA neurons in striatum seen in some transplant paradigms [19].

In summary, we found similarities and differences between fetal- and ES-derived neurons, including DA neurons, in responses to a set of guidance cues. Netrin-1 promoted ES-derived neurite outgrowth via DCC receptor, and Slit1 and Slit3 inhibited ES-derived neuronal outgrowth, which resembled the responses of fetal TH neurites in the same setting. However, neurites from the current protocols of ES differentiation did not react to the chemotropic properties of Netrin-1 and Slit1 and Slit3 molecules in the same way as primary fetal TH neurites. These distinct responses are not well understood. Nonetheless, ES colonies contain multiple cell types not necessarily developed isochronically or patterned normally with specific

regional phenotype-conditioning signals present in the embryo *in vivo*. These differences may point to requirements for new methods and protocols to fully differentiate ES cells to their normal genotypic and phenotypic coding.

Acknowledgements

We are grateful to Dr. Yi Rao for Slit2-expressing cell line and Slit1 and Slit3 plasmids and to Dr. Marc Tessier-Lavigne for Netrin-1-expressing cell line. We also thank Gabriella Brunlid for technical assistance and Dr. S.O. Chan and W.S. Cheung for help with measurements of neurite outgrowth. This study was supported by Udall Parkinson's Disease Research Center of Excellence Grant P50 NS39793, the Michael Stern Parkinson's Disease Research Foundation, and the Orchard and Anti-aging Foundation.

References

1. Simon H, Le Moal M, Calas A. Efferents and afferents of the ventral tegmental-A10 region studied after local injection of [³H]leucine and horseradish peroxidase. *Brain Res* 1979;178:17–40. [PubMed: 91413]
2. Simon H, Le Moal M, Galey D, et al. Silver impregnation of dopaminergic systems after radiofrequency and 6-OHDA lesions of the rat ventral. *Brain Res* 1976;115:215–231. [PubMed: 974747]
3. Colamarino SA, Tessier-Lavigne M. The role of the floor plate in axon guidance. *Annu Rev Neurosci* 1995;18:497–529. [PubMed: 7605072]
4. Hammond R, Vivancos V, Naeem A, et al. Slit-mediated repulsion is a key regulator of motor axon pathfinding in the hindbrain. *Development* 2005;132:4483–4495. [PubMed: 16162649]
5. Lambot MA, Depasse F, Noel JC, et al. Mapping labels in the human developing visual system and the evolution of binocular vision. *J Neurosci* 2005;25:7232–7237. [PubMed: 16079405]
6. Suto F, Ito K, Uemura M, et al. Plexin-a4 mediates axon-repulsive activities of both secreted and transmembrane semaphorins and plays roles in nerve fiber guidance. *J Neurosci* 2005;25:3628–3637. [PubMed: 15814794]
7. Isacson O, Deacon T. Neural transplantation studies reveal the brain's capacity for continuous reconstruction. *Trends Neurosci* 1997;20:477–482. [PubMed: 9347616]
8. Isacson O, Deacon TW. Specific axon guidance factors persist in the adult brain as demonstrated by pig neuroblasts transplanted to the rat. *Neuroscience* 1996;75:827–837. [PubMed: 8951876]
9. Isacson O, Deacon TW, Pakzaban P, et al. Transplanted xenogeneic neural cells in neurodegenerative disease models exhibit remarkable axonal target specificity and distinct growth patterns of glial and axonal fibres. *Nat Med* 1995;1:1189–1194. [PubMed: 7584993]
10. Livesey FJ, Hunt SP. Netrin and netrin receptor expression in the embryonic mammalian nervous system suggests roles in retinal, striatal, nigral, and cerebellar development. *Mol Cell Neurosci* 1997;8:417–429. [PubMed: 9143559]
11. Yue Y, Widmer DA, Halladay AK, et al. Specification of distinct dopaminergic neural pathways: Roles of the Eph family receptor EphB1 and ligand ephrin-B2. *J Neurosci* 1999;19:2090–2101. [PubMed: 10066262]
12. Marillat V, Cases O, Nguyen-Ba-Charvet KT. Spatiotemporal expression patterns of slit and robo genes in the rat brain. *J Comp Neurol* 2002;442:130–155. [PubMed: 11754167]
13. Yasuhara T, Shingo T, Muraoka K, et al. Toxicity of semaphorin3A for dopaminergic neurons. *Neurosci Lett* 2005;382:61–65. [PubMed: 15911122]
14. Lin L, Rao Y, Isacson O. Netrin-1 and slit-2 regulate and direct neurite growth of ventral midbrain dopaminergic neurons. *Mol Cell Neurosci* 2005;28:547–555. [PubMed: 15737744]
15. Thompson L, Barraud P, Andersson E, et al. Identification of dopaminergic neurons of nigral and ventral tegmental area subtypes in grafts of fetal ventral mesencephalon based on cell morphology, protein expression, and efferent projections. *J Neurosci* 2005;25:6467–6477. [PubMed: 16000637]
16. Mendez I, Sanchez-Pernaute R, Cooper O, et al. Cell type analysis of functional fetal dopamine cell suspension transplants in the striatum and substantia nigra of patients with Parkinson's disease. *Brain* 2005;128:1498–1510. [PubMed: 15872020]

17. Allen NJ, Barres BA. Signaling between glia and neurons: Focus on synaptic plasticity. *Curr Opin Neurobiol* 2005;15:542–548. [PubMed: 16144764]
18. Christopherson KS, Ullian EM, Stokes CC, et al. Thrombospondins are astrocyte-secreted proteins that promote CNS synaptogenesis. *Cell* 2005;120:421–433. [PubMed: 15707899]
19. Bjorklund LM, Sanchez-Pernaute R, Chung S, et al. Embryonic stem cells develop into functional dopaminergic neurons after transplantation in a Parkinson rat model. *Proc Natl Acad Sci U S A* 2002;99:2344–2349. [PubMed: 11782534]
20. Baier PC, Schindehutte J, Thinyane K, et al. Behavioral changes in unilaterally 6-hydroxy-dopamine lesioned rats after transplantation of differentiated mouse embryonic stem cells without morphological integration. *STEM CELLS* 2004;22:396–404. [PubMed: 15153616]
21. Sanchez-Pernaute R, Studer L, Ferrari D, et al. Long-term survival of dopamine neurons derived from parthenogenetic primate embryonic stem cells (cyno-1) after transplantation. *STEM CELLS* 2005;23:914–922. [PubMed: 15941857]
22. Zeng X, Cai J, Chen J, et al. Dopaminergic differentiation of human embryonic stem cells. *STEM CELLS* 2004;22:925–940. [PubMed: 15536184]
23. Park CH, Minn YK, Lee JY, et al. In vitro and in vivo analyses of human embryonic stem cell-derived dopamine neurons. *J Neurochem* 2005;92:1265–1276. [PubMed: 15715675]
24. Yurek DM, Fletcher-Turner A. Comparison of embryonic stem cell-derived dopamine neuron grafts and fetal ventral mesencephalic tissue grafts: Morphology and function. *Cell Transplant* 2004;13:295–306. [PubMed: 15191167]
25. Kawasaki H, Mizuseki K, Nishikawa S, et al. Induction of midbrain dopaminergic neurons from ES cells by stromal cell-derived inducing activity. *Neuron* 2000;28:31–40. [PubMed: 11086981]
26. Kim DW, Chung S, Hwang M, et al. Stromal cell-derived inducing activity, Nurr1, and signaling molecules synergistically induce dopaminergic neurons from mouse embryonic stem cells. *STEM CELLS* 2006;24:557–567. [PubMed: 16123386]
27. Sang Q, Wu J, Rao Y, et al. Slit promotes branching and elongation of neurites of interneurons but not projection neurons from the developing telencephalon. *Mol Cell Neurosci* 2002;21:250–265. [PubMed: 12401446]
28. Wu W, Wong K, Chen J, et al. Directional guidance of neuronal migration in the olfactory system by the protein Slit. *Nature* 1999;400:331–336. [PubMed: 10432110]
29. Li HS, Chen JH, Wu W, et al. Vertebrate slit, a secreted ligand for the transmembrane protein roundabout, is a repellent for olfactory bulb axons. *Cell* 1999;96:807–818. [PubMed: 10102269]
30. Shirasaki R, Mirzayan C, Tessier-Lavigne M, et al. Guidance of circumferentially growing axons by netrin-dependent and -independent floor plate chemotropism in the vertebrate brain. *Neuron* 1996;17:1079–1088. [PubMed: 8982157]
31. Metin C, Deleglise D, Serafini T, et al. A role for netrin-1 in the guidance of cortical efferents. *Development* 1997;124:5063–5074. [PubMed: 9362464]
32. de la Torre JR, Hopker VH, Ming GL, et al. Turning of retinal growth cones in a netrin-1 gradient mediated by the netrin receptor DCC. *Neuron* 1997;19:1211–1224. [PubMed: 9427245]
33. Ming GL, Song HJ, Berninger B, et al. cAMP-dependent growth cone guidance by netrin-1. *Neuron* 1997;19:1225–1235. [PubMed: 9427246]
34. Hong K, Hinck L, Nishiyama M, et al. A ligand-gated association between cytoplasmic domains of UNC5 and DCC family receptors converts netrin-induced growth cone attraction to repulsion. *Cell* 1999;97:927–941. [PubMed: 10399920]
35. Zhu Y, Li H, Zhou L, et al. Cellular and molecular guidance of GABAergic neuronal migration from an extracortical origin to the neocortex. *Neuron* 1999;23:473–485. [PubMed: 10433260]
36. Hong K, Hinck L, Nishiyama M, et al. A ligand-gated association between cytoplasmic domains of UNC5 and DCC family receptors converts netrin-induced growth cone attraction to repulsion. *Cell* 1999;97:927–941. [PubMed: 10399920]
37. Braisted JE, Catalano SM, Stimac R, et al. Netrin-1 promotes thalamic axon growth and is required for proper development of the thalamocortical projection. *J Neurosci* 2000;20:5792–5801. [PubMed: 10908620]

38. Deiner MS, Kennedy TE, Fazeli A, et al. Netrin-1 and DCC mediate axon guidance locally at the optic disc: Loss of function leads to optic nerve hypoplasia. *Neuron* 1997;19:575–589. [PubMed: 9331350]
39. Forcet C, Stein E, Pays L, et al. Netrin-1-mediated axon outgrowth requires deleted in colorectal cancer-dependent MAPK activation. *Nature* 2002;417:443–447. [PubMed: 11986622]
40. Kubota C, Nagano T, Baba H, et al. Netrin-1 is crucial for the establishment of the dorsal column-medial lemniscal system. *J Neurochem* 2004;89:1547–1554. [PubMed: 15189358]
41. Kidd T, Bland KS, Goodman CS. Slit is the midline repellent for the robo receptor in *Drosophila*. *Cell* 1999;96:785–794. [PubMed: 10102267]
42. Niclou SP, Jia L, Raper JA. Slit2 is a repellent for retinal ganglion cell axons. *J Neurosci* 2000;20:4962–4974. [PubMed: 10864954]
43. Nguyen-Ba-Charvet KT, Brose K, Marillat V. Slit2-Mediated chemorepulsion and collapse of developing forebrain axons. *Neuron* 1999;22:463–473. [PubMed: 10197527]
44. Nguyen-Ba-Charvet KT, Brose K, Ma L. Diversity and specificity of actions of Slit2 proteolytic fragments in axon guidance. *J Neurosci* 2001;21:4281–4289. [PubMed: 11404413]
45. Wang KH, Brose K, Arnott D, et al. Biochemical purification of a mammalian slit protein as a positive regulator of sensory axon elongation and branching. *Cell* 1999;96:771–784. [PubMed: 10102266]
46. Ming GL, Wong ST, Henley J, et al. Adaptation in the chemotactic guidance of nerve growth cones. *Nature* 2002;417:411–418. [PubMed: 11986620]
47. Kawano H, Horie M, Honma S, et al. Aberrant trajectory of ascending dopaminergic pathway in mice lacking Nkx2.1. *Exp Neurol* 2003;182:103–112. [PubMed: 12821380]
48. Bourikas D, Pekarik V, Baeriswyl T, et al. Sonic hedgehog guides commissural axons along the longitudinal axis of the spinal cord. *Nat Neurosci* 2005;8:297–304. [PubMed: 15746914]

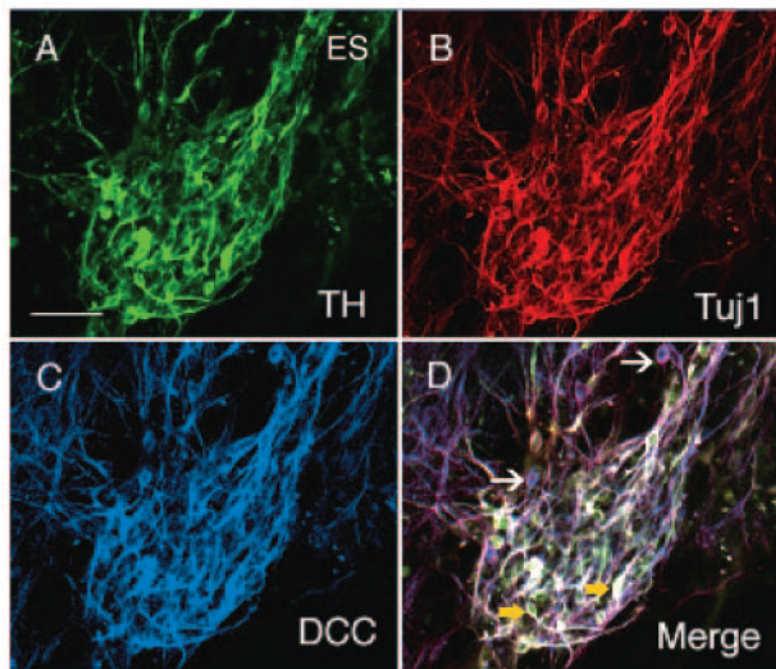
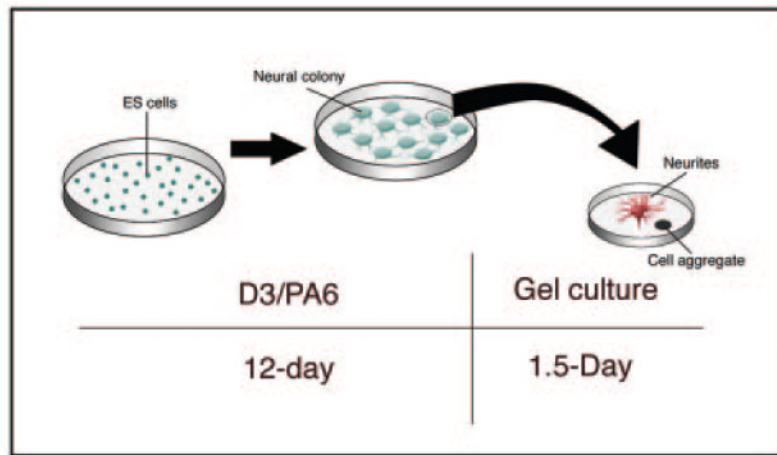


Figure 1.

Culture procedures and DCC expression in ES-derived neurons. Upper panel: Schematic diagram depicting the culture procedures used in the present study. Singular mouse D3 ES cells were seeded on the PA6 stromal cells [25]. Neural colony was formed and was detached for gel culture after a 12-day culture. The neural colony grew neurites after a 1.5-day gel culture. Lower panel: Photomicrograph showing DCC receptor expression in ES-derived neurons. (A): TH. (B): Tuj1. (C): DCC receptor. (D): Merged image showing that DCC receptor is expressed by both TH-positive neurons (yellow arrows) and non-TH neurons (white arrows). Scale bar = 100 μm . Abbreviation: ES, embryonic stem; TH, tyrosine hydroxylase.

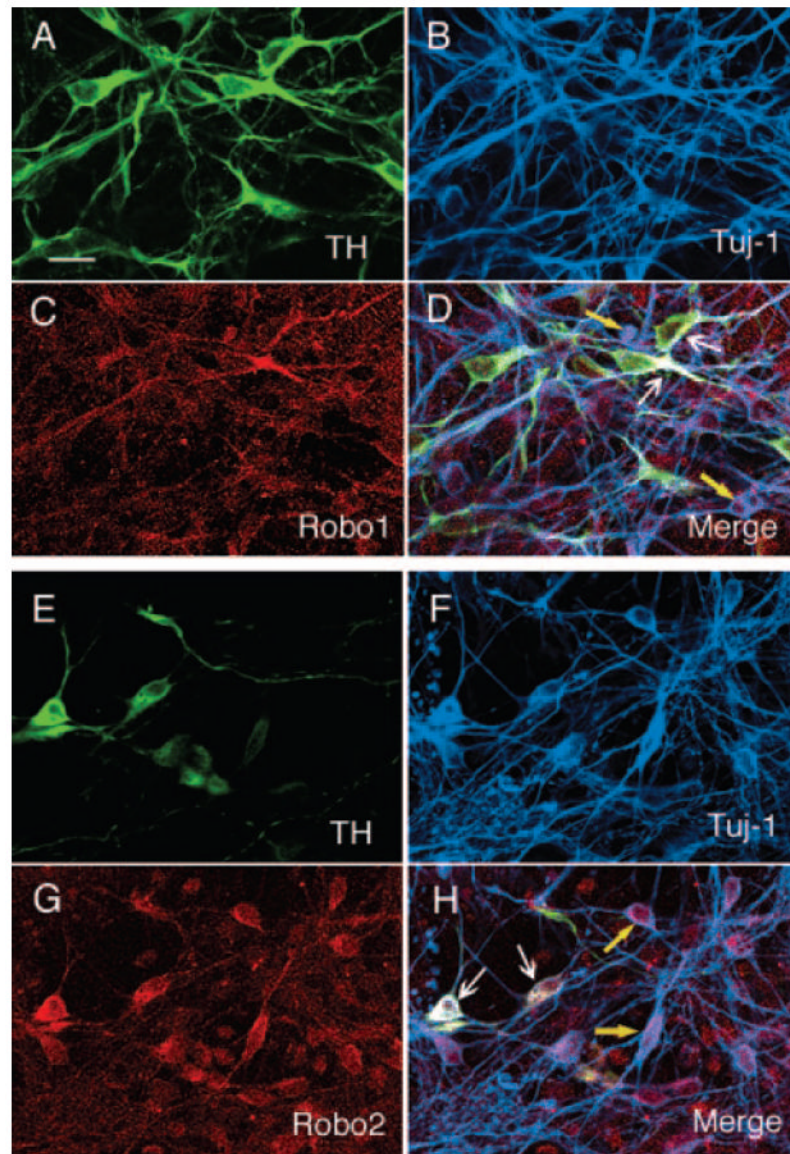


Figure 2. Photomicrograph showing Robo1 and Robo2 receptor expression in embryonic stem cell-derived neurons. **(A):** TH. **(B):** Tuj1. **(C):** Robo1 receptor. **(D):** Merged image showing that Robo1 receptor is present in both TH-positive neurons (white arrows) and non-TH-positive neurons (yellow arrows). **(E):** TH. **(F):** Tuj1. **(G):** Robo2. **(H):** Merged image showing that Robo-2 receptor is expressed by TH-positive neurons (white arrows) and non-TH-positive neurons (yellow arrows). Scale bar = 20 μ m.

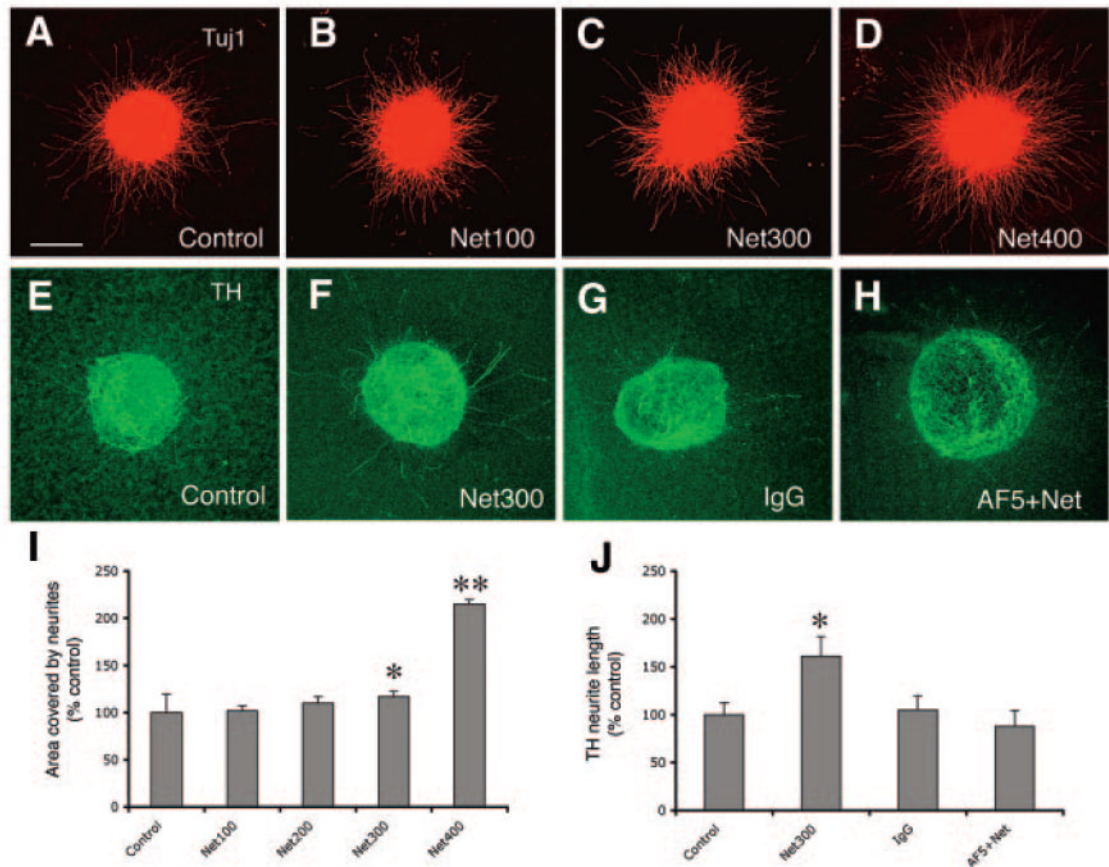


Figure 3.

Netrin-1 protein enhances embryonic stem (ES) neurite outgrowth. (A–D): Tuj1 neurites in the ES explants cultured in the absence of Netrin-1 and in the presence of Netrin-1 at 100, 200, 300, and 400 ng/ml. (E, H): TH neurite growth in explants cultured without netrin-1 protein, with netrin-1 protein, with control IgG and AF5 plus Netrin-1. (I): Tuj1 neurite outgrowth was quantified by measuring area occupied by neurites. Neurite outgrowth is enhanced by Netrin-1 protein in a dose-dependent manner, as Netrin-1 at 300 and 400 ng/ml significantly increases areas covered by neurites compared with control explants (*, $p < .05$; **, $p < .001$). (J): TH neurite length was measured by using NeuroLucida. TH neurite was statistically higher than that in control, IgG-treated, and AF5 plus netrin-1-treated explants (*, $p < .05$). Scale bar = 100 μm . Abbreviation: TH, tyrosine hydroxylase.

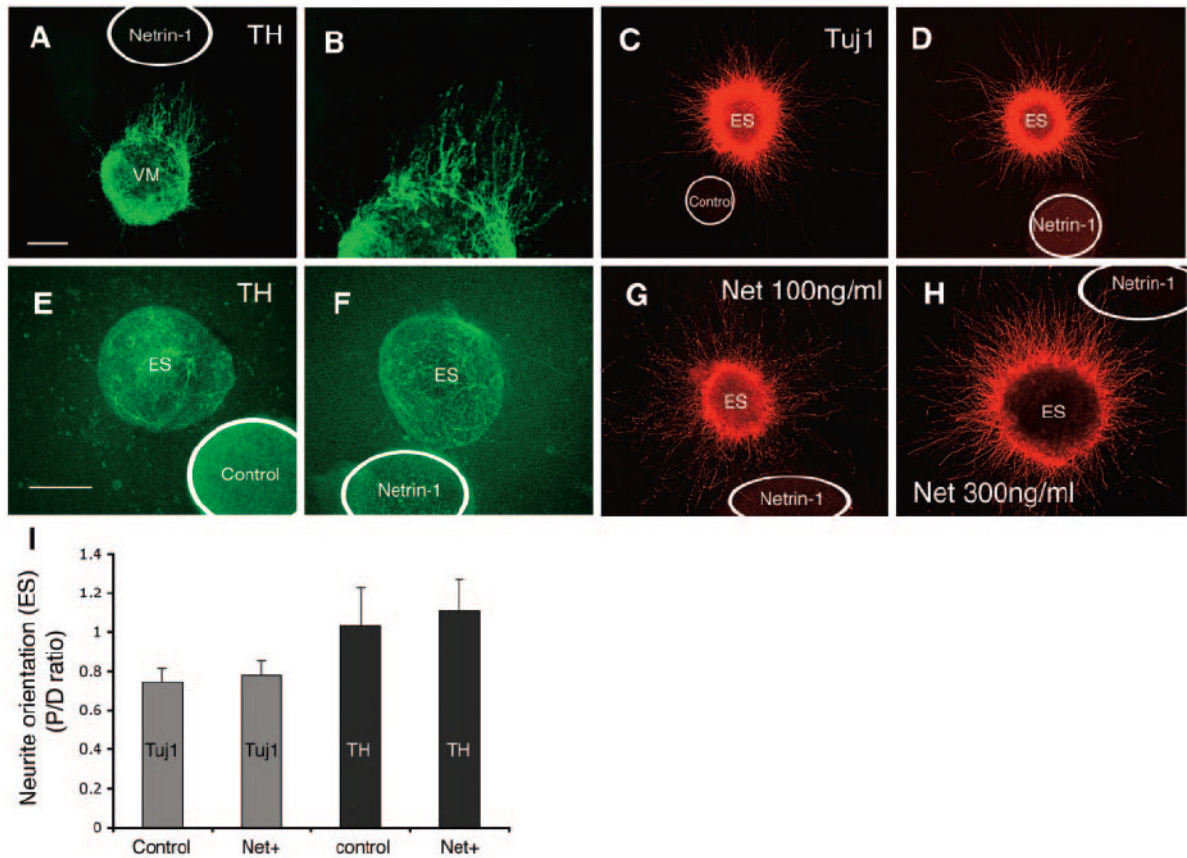


Figure 4.

Neurite outgrowth in cocultures of ES explant with Netrin-1-producing aggregates. (A, B): The majority of TH neurites from E14 ventral midbrain explants cocultured with netrin-1 cells grew toward to netrin-1 cells. (C, D): ES explants cocultured with control cells showed symmetric distribution of Tuj1 neurites, and ES explants cocultured with netrin-1 cells showed symmetric distribution of neurites. (E, F): No steered TH neurite growth was observed in the explants cultured in the absence and in the presence of netrin-1 cells. (G, H): Addition of Netrin-1 protein at 100 and 300 ng/ml to the cocultures of ES cells with netrin-1 aggregates did not change neurite distribution pattern. (I): Areas covered by Tuj1 neurites and numbers of TH neurites in proximal and distal aspect of explants were measured. The ratio of proximal to distal was then calculated. No statistically significant differences were detected between explants cocultured with control cells and explants cocultured with Netrin-1 cells. Scale bar = 100 μ m. Abbreviation: ES, embryonic stem; P/D, proximal/distal; TH, tyrosine hydroxylase.

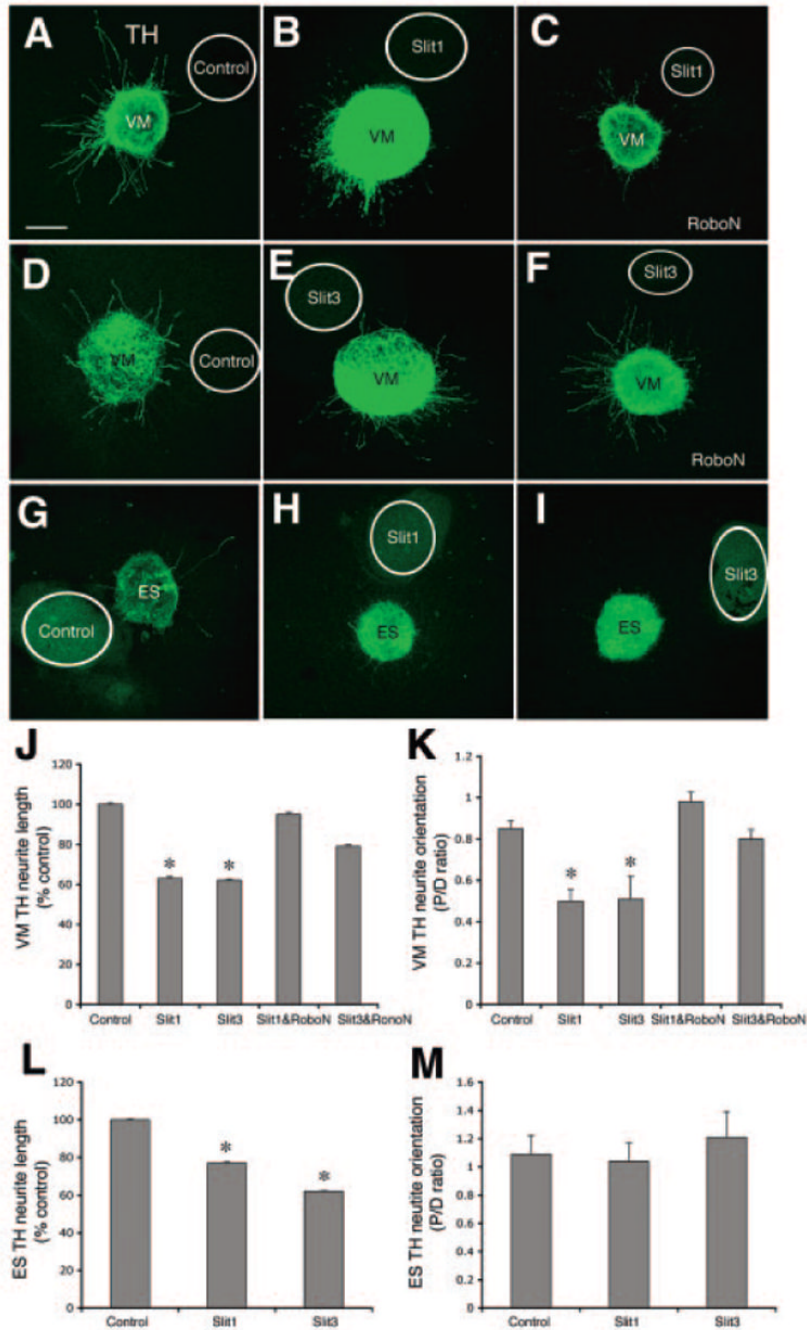


Figure 5. TH neurite outgrowth in cocultures of E14 VM and ES cells with either Slit1- or Slit3-transfected cells. **(A):** Explants cocultured with control cells exhibited nondirected growth. **(B):** The majority of neurites in explants cocultured with Slit1-producing cells was seen in the distal aspects of the explant. **(C):** RoboN at concentration of 1:5 blocked the Slit1-repulsive effect on TH neurites. **(D):** Neurites distributed symmetrically in the explants cultured with control cells. **(E):** Most neurites distributed in the distal part of explants cultured with Slit3 cells. **(F):** RoboN blocked Slit3-repulsive effects on neurite distribution in the explants cultured with Slit3 cells. **(G):** Neurites in the ES explants cultured with control cells. **(H):** Neurites in explants cultured with slit1 cells. **(I):** Neurites in explants cultured with Slit3 cells. **(J):** Neurite

length in VM explants cultured with Slit1 and Slit3 was significantly shorter than that in control explants (*, $p < .001$), and neurite length in RoboN-treated explants cultured with Slit1 and Slit3 did not differ from that in control explants. **(K)**: P/D ratio in VM explants cultured with Slit1 and Slit3 was significantly lower than that in control explant (*, $p < .001$), and P/D ratio in RoboN-treated explants cultured with Slit1 and Slit3 did not differ from that in control explants. **(L)**: ES TH neurite in explants cultured with Slit1 and Slit3 was statistically shorter than that of control explants (*, $p < .01$). **(M)**: P/D ratio in ES explants cultured with Slit1 and Slit3 was not statistically different from that of control explants. Scale bar = 100 μm . Abbreviations: ES, embryonic stem; P/D, proximal/distal; TH, tyrosine hydroxylase; VM, ventral midbrain.

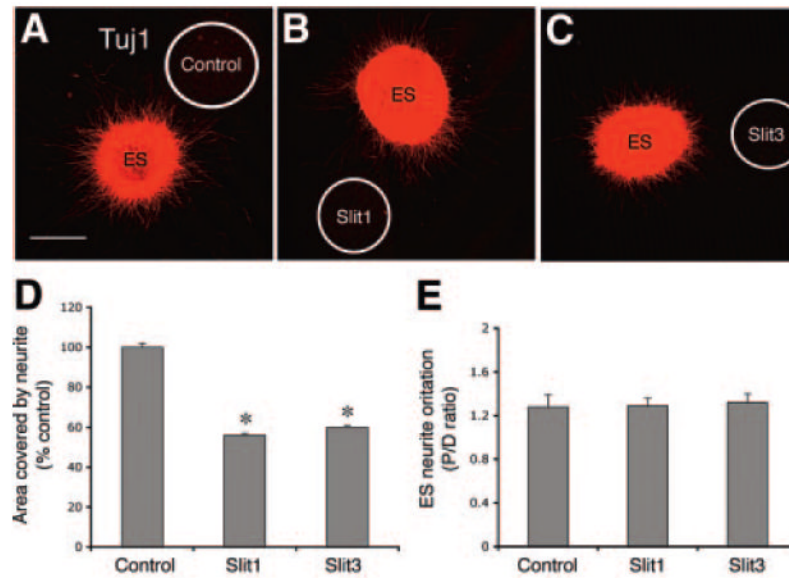


Figure 6. Effects of Slit1 and Slit3 on Tuj1 neurite outgrowth of ES explants. (A–C): Tuj1 neurite outgrowth in ES explants cultures with control cells, Slit1-transfected cells, and Slit3-transfected cells, respectively. The area covered by neurite in the proximal and distal part of explant was measured, and the P/D ratio was then calculated. (D): Statistical analysis shows that area covered by explants cultured with Slit1 or Slit3 transfected cells was significantly lower than that of control explants (*, $p < .001$). (E): Statistical analysis shows no significant difference of the P/D ratio found between control explants and explants cultured with Slit1 or Slit3 cells. Scale bar = 100 μm . Abbreviations: ES, embryonic stem; P/D, proximal/distal.

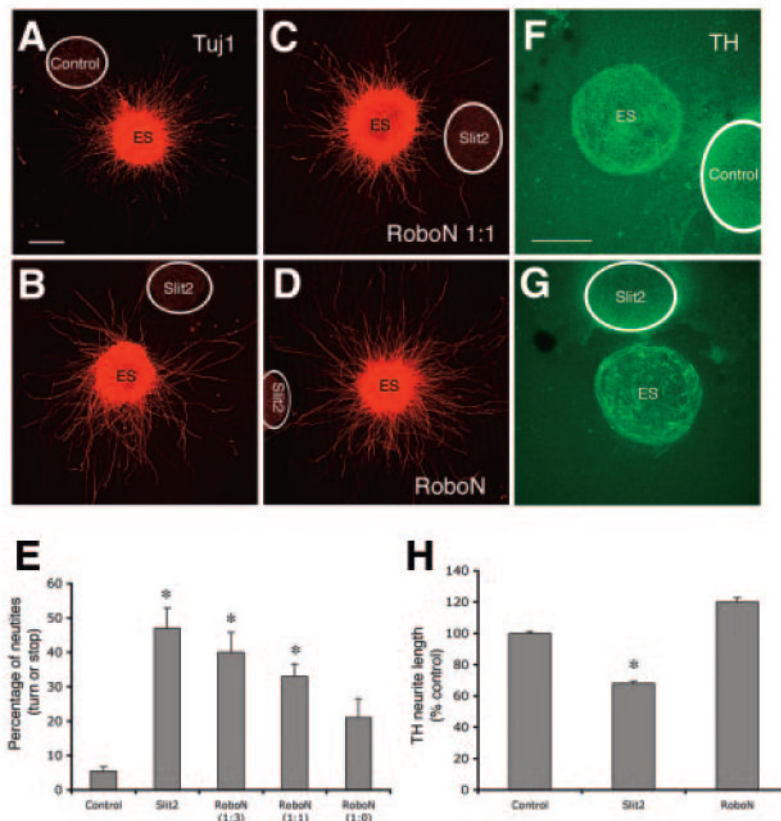


Figure 7.

Effects of Slit2 on neurite outgrowth of ES-derived neurons. **(A–D)**: Tuj1 neurite outgrowth in ES explants cultured with control cells, Slit2-expressing cells only, and Slit2 cells plus conditioned medium RoboN added to the cultures at dilution of 1:1 and 1:0. **(E)**: Neurites of the proximal explant that stop or turn away from the aggregates were counted and are presented as percentage of total neurite counted. Statistical analysis reveals that percentage of stop or turn in the explants cultured with Slit2 with addition of RoboN at 1:3 and 1:1 was significantly greater than that of control explants (*, $p < .01$), whereas the percentage in the RoboN (1:0)-treated explants did not differ from that of control explants. **(F, G)**: TH neurite outgrowth in ES explants cultured with control and Slit2 cells. **(H)**: TH neurite outgrowth was inhibited by Slit2 cells and could be reversed by addition of RoboN (* $p < .05$). Scale bar = 100 μm . Abbreviation: ES, embryonic stem; TH, tyrosine hydroxylase.